Error Scaling in Position Estimation from Noisy Relative Pose Measurements

Joseph Knuth and Prabir Barooah

Technical Report

***Abstract*—We examine how fast the estimation error grows with time when a mobile robot/vehicle estimates its location from relative pose measurements without global position or orientation sensors. We show that both bias and variance of the position estimation error grows at most linearly with time (or distance traversed) asymptotically. The bias growth rate is crucially dependent on the trajectory of the robot. An exact formula for the error bias is provided for a special case of a periodic trajectory in 2-D. Experiments with a P3-DX wheeled robot and Monte-Carlo simulations are provided to verify the theoretical predictions.**

I. Introduction

Localization without GPS is a key capability for autonomous robots, since there are many situations in which GPS signals are either unavailable or only intermittently available. These include operation in urban canyons and tunnels, inside buildings, under water, and extra-planetary exploration. In such a situation, localization with respect to an initial position is typically performed using a combination of sensors that are used to measure relative motion between two successive time instants, and then chaining them together. Inertial sensors (gyroscopes and accelerometers), vision-based sensors (cameras, LIDARs, etc) and joint encoders (in case of ground vehicles) are examples of sensors that can be used to obtain such measurements. Apart from robotic platforms, such localization is also of relevance to human wearable systems [1], personal navigation devices [2], and robot end-effector position estimation [3].

When relative motion measurements obtained from sensors are concatenated to form an estimate of the robot's position in a global frame, errors in individual measurements accumulate. Over long time horizons, the resulting location estimates may become quite poor. A number of papers have examined the question of how the error varies with time in such a situation. Olson et. al. [4] states that without a global orientation sensor, the error grows super-linearly with distance, and presents experimental evidence. They also state that position estimation error will grow as $O(s^{3/2})$, where s is the distance travelled. Roumeliotis *et. al.* [5] examine the error growth in cooperative localization with multiple robots moving in a 2-D plane, in which each robot is equipped with an absolute orientation sensor. They examine the 2-D scenario, in which each robot's motion is restricted to a 2-D plane and its pose is described by a triple (x, y, θ), where x, y are the X- and Y-coordinates of the origin of the local coordinate frame of the robot in the global frame and θ, the orientation, is the angle between the X-axis of the local frame and the X-axis of the global frame. It follows from the results in [5] that for the scenario examined, the covariance of a robot's position estimation error grows linearly with time.

In this paper we examine the growth rate in the position estimation error of a robot that cannot directly measure either its global position or its global orientation. The robot is equipped with sensors that allows it to measure the relative pose (position and orientation) between its coordinate frames at two successive time instants, but not sensors that can measure its absolute pose with respect to a global coordinate frame. That is, the robot may have sensors such as wheel odometers and cameras, but does not have sensors such as GPS and compasses. The absolute position has to be estimated from the noisy relative pose measurements.

We show that in the general d-D case, (when the robot's pose is an element of $SE(d)$) both the bias and variance in the position estimation error grows at most linearly with time. Thus, even without an absolute orientation sensor, the error growth (both bias and variance) is at most linear. This is a generalization of the result in [5] which assumed availability of absolute orientation sensors and examined only the 2-D scenario. Our results are in contrast to the superlinear growth of error reported in [4].

The growth in the bias depends crucially on the type of path the robot traverses. In particular, we show that if the robot stays within a bounded region, then the bias in the error is also bounded by a constant. We also provide a formula for the bias of the position estimation error in the special case when the robot moves in a periodic trajectory in 2-D. In the 2-D case its pose is described by the triple (x, y, θ). This prediction is verified numerically through Monte-Carlo simulations and experiments conducted with a Pioneer P3-DX robot equipped with a vision-based sensor and a wheel odometer.

The rest of the paper is organized as follows. Section I-A discusses some related work. Section II precisely formulates the problem under study, and Section III states the main results. Most of the proofs are in the appendix at the end of the paper. Simulation verification is presented in Section IV and experimental verification is presented in Section V. The paper ends with a discussion of the results in Section VI.

A. Related work

The papers by Smith and Cheesman [3], Su and Lee [6], and Wang and Chirikjian [7] derived recursive expressions of the covariance of the pose estimation error by assuming the errors are small, so that a first order approximation of the

BCH (Baker-Campbell-Hausdorff) formula is valid. Recently, Wang and Chirikjian [8] developed a recursive formula for the covariance of the pose estimation error that retains the second order terms in the BCH formula. These papers study the covariance of a six-dimensional vector whose entries describe the robot's pose (they are the coefficients of the six-dimensional basis of $SE(3)$). However, they do not directly examine the mean and covariance of the position estimation error.

A related body of literature deals with state estimation of systems whose states, as well as the noisy measurements, are in $SO(3)$ or $SE(3)$ (see [9], [10] and references therein). The problem of position estimation of a mobile robot with noisy relative pose measurements between successive frames - one that is central to this paper - falls into this category. However, our aim is not to develop an estimation technique, but to examine the growth of error in the position estimate when successive noisy relative pose measurements are chained together to obtain a global pose estimate.

II. Problem statement

We measure time with a discrete index $k = 0, 1, \ldots$. Sensors used for relative localization of robots yield an estimate of the position and orientation of the robot at time k relative to that in the previous time instant, $k-1$. That is, they produce an estimate of the *relative pose* between frames attached to the robot at two successive time instants. Let ${}^{k}_{k+1}\mathbf{R}$ be the rotation between the local frames attached to the robot's body at time k and $k+1$. That is, if ${}^{k}\mathbf{u}$ is a vector expressed in the robot's frame at time k and ${}^{k-1}\mathbf{u}$ is the same vector expressed in the robot's frame at time $k-1$, then ${}^{k-1}\mathbf{u} = {}^{k-1}_{k}\mathbf{R}\ {}^{k}\mathbf{u}$. We will refer to the frame that is attached to the robot at time k as the "frame k". Similarly, let ${}^{k}\mathbf{t}_{i,j}$ be the relative translation from the frame i to the frame j, expressed in the frame k. The rotation ${}^{k-1}_{k}\mathbf{R} \in \mathrm{SO}(d)$ is usually expressed as a $d \times d$ matrix for $d \geq 2$, while ${}^{k}\mathbf{t}_{i,j}$ is a vector in $\mathbb{R}^2$ or $\mathbb{R}^3$. Without loss of generality, the coordinate frame that is attached to the robot's body at the initial time $k = 0$ is used as the global coordinate frame. We denote the rotation from frame k to the global reference frame (frame 0) by ${}^{0}_{k}\mathbf{R}$. Similarly, the translation from frame $k-1$ to k expressed in the global reference frame is denoted by ${}^{0}\mathbf{t}_{k-1,k}$. The position of the robot at time n is the vector ${}^{0}\mathbf{t}_{0,n}$.

A. Pose estimation from relative measurements

With relative pose sensors such as cameras, inertial sensors, and wheel odometers, the measurements available at time k are estimates of the relative translation from $k-1$ to frame k expressed in frame k, i.e., of ${}^{k}\mathbf{t}_{k-1,k}$, and the rotation between the frames $k-1$ and k. i.e., of ${}^{k-1}_{k}\mathbf{R}$. The translation from $k-1$ to k, for $k \geq 1$, expressed in the global reference frame is

$$ {}^{0}\mathbf{t}_{k-1,k} = {}^{0}_{k}\mathbf{R}\,{}^{k}\mathbf{t}_{k-1,k}, \text{ where } {}^{0}_{k}\mathbf{R} \quad = {}^{0}_{1}\mathbf{R}\,{}^{1}_{2}\mathbf{R} \ldots {}^{k-1}_{k}\mathbf{R}. $$

Estimates are denoted by hats on top of the corresponding symbol, and errors by tildes, so that ${}^{k-1}_{k}\hat{\mathbf{R}}$ and ${}^{k}\hat{\mathbf{t}}_{k-1,k}$ are the noisy estimates of ${}^{k-1}_{k}\mathbf{R}$ and ${}^{k}\mathbf{t}_{k-1,k}$, respectively, and the corresponding errors ${}^{k-1}_{k}\tilde{\mathbf{R}}$ and ${}^{k}\tilde{\mathbf{t}}_{k-1,k}$ are defined as

$$ \begin{aligned} {}^{k-1}_{k}\tilde{\mathbf{R}} &:= ({}^{k-1}_{k}\mathbf{R})^{-1}\,{}^{k-1}_{k}\hat{\mathbf{R}}, \\ {}^{k}\tilde{\mathbf{t}}_{k-1,k} &:= {}^{k}\hat{\mathbf{t}}_{k-,k} - {}^{k}\mathbf{t}_{k-1,k}. \end{aligned} \tag{1} $$

The mean and the covariance of the translation errors are denoted as: $\mathrm{E}[{}^{k}\tilde{\mathbf{t}}_{k-1,k}] =: \mathbf{b}_k$ and $Cov({}^{k}\tilde{\mathbf{t}}_{k-1,k}, {}^{k}\tilde{\mathbf{t}}_{k-1,k}) =: \mathbf{P}_k$. The absolute position of the robot at time k is determined by adding the relative position measurements, after expressing them all in the global coordinate frame. The measurement of the translation from frame $k-1$ to k expressed in the global reference frame, which is denoted by ${}^{0}\hat{\mathbf{t}}_{k-1,k}$, is

$$ {}^{0}\hat{\mathbf{t}}_{k-1,k} := {}^{0}_{k}\hat{\mathbf{R}}\,{}^{k}\hat{\mathbf{t}}_{k-1,k}, \tag{2} $$

where ${}^{0}_{k}\hat{\mathbf{R}}$ is an estimate of ${}^{0}_{k}\mathbf{R}$, which is computed from the relative rotation estimates as

$$ {}^{0}_{k}\hat{\mathbf{R}} = \prod_{i=1}^{k} {}^{i-1}_{i}\hat{\mathbf{R}}. \tag{3} $$

Finally, the estimate of the position at time n in the global reference frame is obtained by adding the relative translation estimates:

$$ {}^{0}\hat{\mathbf{t}}_{0,n} := \sum_{k=1}^{n} {}^{0}\hat{\mathbf{t}}_{k-1,k} = \sum_{k=1}^{n} \left({}^{0}_{k}\hat{\mathbf{R}}\ \ {}^{k}\hat{\mathbf{t}}_{k-1,k} \right) \tag{4} $$

The error between the estimated position and the true position at time n is

$$ \mathbf{e}(n) := {}^{0}\mathbf{t}_{0,n} - {}^{0}\hat{\mathbf{t}}_{0,n}. \tag{5} $$

Our goal is to study how the mean and covariance of the position estimation error $\mathbf{e}(n)$ scales with the time index n.

Remark 1: We wish to emphasize that the estimation error resulting from the estimation method described above will have the same asymptotic trend as that of a filtering technique that uses a kinematic model of the robot motion. The reason is that a kinematic model essentially produces an independent noisy measurement of the relative pose. Thus, our investigations are useful in analyzing asymptotic performance of a wider class of estimation techniques. □

To address the issue of statistical dependencies among the measurement errors, we establish a few conventions. A rotation matrix $R \in SO(d)$ can be represented by the exponential map: $R = e^{\omega^s}$, where ω^s is the skew-symmetric matrix corresponding to the vector $\omega \in \mathbb{R}^d$ [11]. A random rotation matrix $\mathbf{R}$ can therefore be specified by a d-dimensional random vector $\boldsymbol{\omega}$. We say that two random rotation matrices $\mathbf{R}_1$ $(= e^{\boldsymbol{\omega}_1^s})$ and $\mathbf{R}_2$ $(= e^{\boldsymbol{\omega}_2^s})$ are independent if $\boldsymbol{\omega}_1$ and $\boldsymbol{\omega}_2$ are independent random vectors. Similarly, we say that $\mathbf{R}_1$ and a random vector $\mathbf{t}$ are independent if $\boldsymbol{\omega}_1$ and $\mathbf{t}$ are independent random vectors. In the first case every entry of the matrix $\mathbf{R}_1$ is independent of every entry of $\mathbf{R}_2$, and in the second case, of every entry of $\mathbf{t}$. In this paper, we use $\mathrm{E}[\mathbf{R}]$ (for a random rotation matrix $\mathbf{R}$) to denote the matrix whose i,j-th entry is

$\mathrm{E}[(\mathbf{R})_{i,j}]$, i.e., the expected value of the i,j-th entry of $\mathbf{R}$. As a result of this convention, if $\mathbf{R}_1 \in SO(d)$ is independent of $\mathbf{R}_2 \in SO(d)$ and of $\mathbf{t} \in \mathbb{R}^3$, then $\mathrm{E}[\mathbf{R}_1\mathbf{R}_2] = \mathrm{E}[\mathbf{R}_1]\,\mathrm{E}[\mathbf{R}_2]$ and $\mathrm{E}[\mathbf{R}_1\mathbf{t}] = \mathrm{E}[\mathbf{R}_1]\,\mathrm{E}[\mathbf{t}]$. In the sequel, $\|\cdot\|_q$ denotes the (induced) q-norm of a (matrix) vector. When the subscript is omitted, it denotes the (induced) 2-norm.

Remark 2: According to the convention used in this paper, in general $\mathrm{E}[\mathbf{R}] \notin SO(d)$ even if $\mathbf{R} \in SO(d)$. It is important that the notation $\mathrm{E}[\mathbf{R}]$ is not to be understood as the expectation of the random variable $\mathbf{R}$ with a distribution defined over $SO(d)$, in which case its expected value is also an element of $SO(d)$. Even when $\mathbf{R}$ and $\mathbf{t}$ are independent, the equation $\mathrm{E}[\mathbf{R}\mathbf{t}] = \mathrm{E}[\mathbf{R}]\,\mathrm{E}[\mathbf{t}]$ may not hold in general if $\mathrm{E}[\mathbf{R}] \in SO(d)$. □

We state the following assumptions for use in the rest of the paper:

Assumption 1:
1) The relative orientation measurement errors ${}^{k}_{k+1}\tilde{\mathbf{R}}$ are i.i.d. with a non-degenerate distribution. That is, if $\mathbf{R}$ is a random rotation matrix that has the same distribution as each of the ${}^{k}_{k+1}\tilde{\mathbf{R}}$'s, then the distribution of $\mathbf{R}$ is not concentrated in one point in $SO(d)$.
2) The relative translation measurement errors $\{{}^{k}\tilde{\mathbf{t}}_{k-1,k}\}_{k=1}^{\infty}$ are uniformly absolutely integrable, i.e., there exists $\beta > 0$ so that $\beta_k \leq \beta < \infty$ for all k where $\beta_k := \mathrm{E}\,\|{}^{k}\tilde{\mathbf{t}}_{k-1,k}\|$.

Assumption 2:
1) There exist positive constants τ, b, $\underline{p}$, $\overline{p}$ such that $\|{}^{k}\mathbf{t}_{k-1,k}\| \leq \tau$, $\|\mathbf{b}_k\| \leq b$, and $0 < \underline{p} \leq \mathrm{Tr}\,[\mathbf{P}_k] \leq \overline{p} < \infty$ for all k, where $\mathrm{Tr}\,[\cdot]$ stands for trace.
2) The relative translation measurement errors $\{{}^{k}\tilde{\mathbf{t}}_{k-1,k}\}_{k=1}^{\infty}$ is a sequence of an independent random vectors.
3) The rotation and translation measurement errors ${}^{j-1}_{j}\tilde{\mathbf{R}}$ and ${}^{k}\tilde{\mathbf{t}}_{k-1,k}$ are independent if $j \neq k$, and possibly dependent when $j = k$, with $\mathrm{E}[{}^{k-1}_{k}\tilde{\mathbf{R}}\,{}^{k}\tilde{\mathbf{t}}_{k-1,k}] =: \boldsymbol{\rho}_k \in \mathbb{R}^d$. There exists a positive scalar ρ such that $\|\boldsymbol{\rho}_k\| \leq \rho$ for all k.

The assumption $\|{}^{k}\mathbf{t}_{k-1,k}\| \leq \tau$ means that the speed of the robot is upper bounded by a constant. Note that it is *not* assumed that the relative translation and rotation measurement errors at a particular time instant are statistically independent. In practice, they are likely to be dependent if there is overlap between the sensor suite used to measure these two components of the relative pose.

III. Error scaling

For future we use, we define $\bar{\mathbf{R}} = \mathrm{E}[\mathbf{R}]$ and $\gamma := \bar{\mathbf{R}}$. Recall that $\mathbf{R}$ has the same distribution as each of the ${}^{k}_{k+1}\tilde{\mathbf{R}}$'s. It should be noted that $\bar{\mathbf{R}} \notin SO(2)$, and $\gamma < 1$ (see Proposition 1 in the Appendix). The next theorem is the main result of the paper.

Theorem 1: Under Assumption 1 and 2, we have $\big|\|{}^{0}\mathbf{t}_{0,n}\| - a\big| \leq \|\,\mathrm{E}[\mathbf{e}(n)]\| = \|{}^{0}\mathbf{t}_{0,n}\| + a$, where a is a positive constant independent of n, and $\mathrm{Tr}\,[Cov(\mathbf{e}(n),\mathbf{e}(n))] = O(n)$. If $\underline{p} \geq 2b\tau + \tau^2 + 2\dfrac{(\tau+\rho/\gamma)(\tau+b)}{1-\gamma}$, where b, ρ, τ are as defined in Assumption 2, then $\mathrm{Tr}\,[Cov(\mathbf{e}(n),\mathbf{e}(n))] = \Theta(n)$. □

Remark 3: Theorem 1 implies that the bias of the position estimation error grows with time asymptotically at the same rate as the robot's displacement. It follows that if the robot moves with a constant speed and with a constant (absolute) orientation, then its bias grows linearly with time: $\|\,\mathrm{E}[\mathbf{e}(n)]\| = \Theta(n)$. If the robot's motion is confined to a bounded region of the 2-D plane, the bias in its position estimation error stays uniformly bounded by a constant: $\|\,\mathrm{E}[\mathbf{e}(n)]\| = O(1)$. The variance growth rate is not dependent on the trajectory of the robot. In addition, it follows from the theorem that both bias and variance in the position estimation error grows at most linearly with time. The same conclusion is true for error growth with distance, if the speed of the robot is both upper and lower bounded by two constants. These results are in contrast to the prevalent belief in the literature [4] that the error growth is superlinear in time when absolute position measurements are unavailable. Some insight into this belief can be gained by noting that this theorem gives no guarantee on the growth rates over any finite time. Thus the growth rates may appear superlinear when examined over shorter time scales. Although we do not present here due to lack of space, the error growth when the robot moves in a straight line do appear to grow superlinearly with time for small values of time index n; the linear asymptotics become clear only for very large values of n (see [12] for details). □

The proof of Theorem 1 will require the following result, whose proof is provided in the Appendix.

Lemma 1: Under Assumption 1 and 2, we have

$$\|\,\mathrm{E}[{}^{0}\hat{\mathbf{t}}_{0,n}]\| = O(1), \qquad \mathrm{E}[({}^{0}\hat{\mathbf{t}}_{0,n})^T\ {}^{0}\hat{\mathbf{t}}_{0,n}] = O(n).$$

Moreover, if $\underline{p} \geq 2b\tau + \tau^2 + 2\dfrac{(\tau+\rho/\gamma)(\tau+b)}{1-\gamma}$, then we have $\mathrm{E}[({}^{0}\hat{\mathbf{t}}_{0,n})^T\ {}^{0}\hat{\mathbf{t}}_{0,n}] = \Theta(n)$. □

Proof of Theorem 1: It follows from (5), by applying the triangle inequality that

$$\|\,\mathrm{E}[\mathbf{e}(n)]\| \leq \|{}^{0}\mathbf{t}_{0,n}\| + \|\,\mathrm{E}[{}^{0}\hat{\mathbf{t}}_{0,n}]\| \tag{6}$$

$$\|\,\mathrm{E}[\mathbf{e}(n)]\| \geq \Big|\|{}^{0}\mathbf{t}_{0,n}\| - \|\,\mathrm{E}[{}^{0}\hat{\mathbf{t}}_{0,n}]\|\Big| \tag{7}$$

From Lemma 1, we have that $\|\,\mathrm{E}[{}^{0}\hat{\mathbf{t}}_{0,n}]\|$ is upper bounded by a constant independent of n. Calling this upper bound a, the first statement follows immediately from (6) and (7).
To prove the second statement, note that

$$\begin{aligned}\mathrm{Tr}\,[Cov(\mathbf{e}(n),\mathbf{e}(n))] &= \mathrm{Tr}\left[Cov({}^{0}\hat{\mathbf{t}}_{0,n},\ {}^{0}\hat{\mathbf{t}}_{0,n})\right]\\ &= \mathrm{Tr}\left[\mathrm{E}[{}^{0}\hat{\mathbf{t}}_{0,n}({}^{0}\hat{\mathbf{t}}_{0,n})^T] - \mathrm{E}[{}^{0}\hat{\mathbf{t}}_{0,n}]\,\mathrm{E}[{}^{0}\hat{\mathbf{t}}_{0,n}]^T\right]\\ &= \mathrm{E}[({}^{0}\hat{\mathbf{t}}_{0,n})^T\,{}^{0}\hat{\mathbf{t}}_{0,n}] - \|\,\mathrm{E}[{}^{0}\hat{\mathbf{t}}_{0,n}]\|^2\end{aligned}$$

Since $\|\,\mathrm{E}[{}^{0}\hat{\mathbf{t}}_{0,n}]\| = O(1)$, the second statement follows from Lemma 1. ■

A. Special case(s) in 2-D

In this section we provide non-asymptotic results on the error growth for the special case when the motion of the robot is confined to a 2D plane and its trajectory is limited a certain type(s). Note that in this "2-D scenario", ${}^{i}\hat{\mathbf{t}}_{j,k}, {}^{i}\mathbf{t}_{j,k} \in \mathbb{R}^2$ and ${}^{i}_{j}\mathbf{R}, {}^{i}_{j}\hat{\mathbf{R}} \in SO(2)$ for every i, j, k. Without loss of generality, the robot's motion is assumed to lie in the plane formed by this reference frame's x and y axes. The robot's orientation at time n can then be uniquely described by an angle $\theta_{0,n} \in [-\pi,\ \pi)$, which describes rotation of its local frame about the z-axis of the global frame. The relative rotation between the frames $k-1$ and k is uniquely determined by the angle by which the frame $k-1$ has to be rotated in the counter clockwise direction to reach frame k, which we denote by $\theta_{k-1,k}$. Figure 1 shows an example. A noisy measurement of the relative rotation, denoted by $\hat{\theta}_{k-1,k}$, is assumed available at time k. The error in the relative rotation measurement is

$$\tilde{\theta}_{k-1,k} := \hat{\theta}_{k-1,k} - \theta_{k-1,k}. \tag{8}$$

For future use, we define $f_R : [-\pi, \pi) \to SO(2)$ as

$$f_R(\alpha) := \begin{pmatrix} \cos\alpha & -\sin\alpha \\ \sin\alpha & \cos\alpha \end{pmatrix}.$$

The matrix ${}^{k-1}_{k}\mathbf{R}$ that describes the relative rotation between the frames $k-1$ and k is therefore given by ${}^{k-1}_{k}\mathbf{R} = f_R(\theta_{k-1,k})$. It can be shown from the definition (1) that

$${}^{k-1}_{k}\tilde{\mathbf{R}} = f_R(\tilde{\theta}_{k-1,k}). \tag{9}$$

The estimate of the rotation ${}^{k-1}_{k}\mathbf{R}$ therefore is ${}^{k-1}_{k}\hat{\mathbf{R}} = f_R(\hat{\theta}_{k-1,k})$.

We say the robot moves in a *periodic trajectory with period* p if the absolute orientation and position of the robot satisfies the following conditions: $\theta_{0,k} = \theta_{0,k+p}$ and ${}^{0}\mathbf{t}_{0,k} = {}^{0}\mathbf{t}_{0,k+p}$ for all k. The shape of the (closed) path along which the robot moves can be arbitrary. In the statement of the theorem presented next, η denotes the number of periods up to time n, and q to denote the residual, i.e., $\eta(n) := \lfloor n/p \rfloor$ and $q := n - \eta p$. The proof of the result is provided in the Appendix.

Theorem 2: Suppose a robot is moving in $\mathbb{R}^2$ whose trajectory is periodic with period p, and Assumption 1 holds. Suppose that in addition, the distribution of $\tilde{\theta}$ is symmetric around its mean $\mathrm{E}[\tilde{\theta}]$, and the fist moments of the measurement errors are periodic with period p (so that $\boldsymbol{\rho}_k = \boldsymbol{\rho}_{k+p}$). In that case,

$$\begin{aligned}\mathrm{E}[\mathbf{e}(n)] = {}^{0}\mathbf{t}_{0,q} - (I - (c\underline{\mathbf{R}})^p)^{-1} \\ \times (I - (c\underline{\mathbf{R}})^{\eta p})\, w(p) - (c\underline{\mathbf{R}})^{\eta p} w(q),\end{aligned} \tag{10}$$

where

$$c := \mathrm{E}[\cos\left(\tilde{\theta} - \mathrm{E}[\tilde{\theta}]\right)], \qquad \underline{\mathbf{R}} := f_R(\mathrm{E}[\tilde{\theta}]), \tag{11}$$

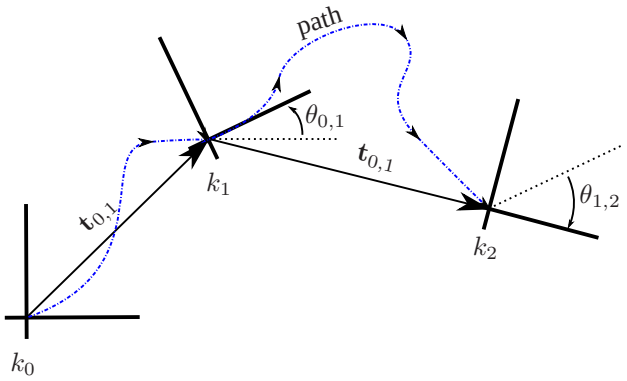

Fig. 1. An example of a robot's path (shown in blue) in 2-D and associated relative poses between time instants.

and $w(j)$ is given by

$$w(j) := \sum_{i=0}^{j-1} (c\underline{\mathbf{R}})^{i}\, {}^{0}_{i+1}\mathbf{R} \left(c\underline{\mathbf{R}}\, {}^{i+1}\mathbf{t}_{i,i+1} + \boldsymbol{\rho}_i\right).$$

Note that $|c| < 1$ since the r.v. $\tilde{\theta}$ is not concentrated at 0 (see Proposition 1 in the Appendix). The spectral radius of $c\underline{\mathbf{R}}$ is strictly lower than unity since $c < 1$ and $\underline{\mathbf{R}} \in SO(2)$. Hence $I - c\underline{\mathbf{R}}$ is invertible and the right-hand side in (10) is well defined.

The assumption of the moments $\boldsymbol{\rho}_k$ being periodic with period p is motivated by the use of vision-based sensors to measure relative poses. In that case the measurement error statistics may depend on the scene the camera sees, which will repeat itself every p instants due to the periodic nature of the robot's motion. Note that i.i.d. errors are a special case of errors with periodic statistics, so the result also holds if all the measurement errors are i.i.d. It follows from (10) that the bias is $O(1)$ (due to $|c| < 1$), which is consistent with Theorem 1.

We can also derive non-asymptotic expressions for the bias and variance of the position estimation error when the robot moves in a straight line; the interested reader is referred to [12] for details.

The next result is on the position estimation error growth rate when the robot moves in a straight line with constant velocity and orientation. The proof of the result is in the Appendix.

Theorem 3: Consider a robot that moves on a 2-D plane in such a manner that for all k, $\theta_{k-1,k} = 0$ and ${}^{k}\mathbf{t}_{k-1,k} = \mathbf{r} \in \mathbb{R}^2$, for some vector $\mathbf{r}$. Suppose that in addition to Assumptions 1 and 2, the distribution of $\tilde{\theta}$ is symmetric around its mean $\mathrm{E}[\tilde{\theta}]$, $\{{}^{k}\tilde{\mathbf{t}}_{k-1,k}\}_{k=1}^{\infty}$ is wide sense stationary with $\mathbf{b} = \mathbf{b}_k$, $\mathbf{P} = \mathbf{P}_k$, and $\boldsymbol{\rho}_k = \boldsymbol{\rho}$ for all k. In that case, we have

$$\begin{aligned}&\mathrm{E}[\mathbf{e}(n)] = n\,\mathbf{r} - (I - c\underline{\mathbf{R}})^{-1}\,(I - (c\underline{\mathbf{R}})^n)\,(c\underline{\mathbf{R}}\mathbf{r} + \boldsymbol{\rho}) \\ &\mathrm{Tr}\,[Cov(\mathbf{e}(n), \mathbf{e}(n))] = \psi n + \omega(n),\end{aligned} \tag{13}$$

where

$$c := \mathrm{E}[\cos\left(\tilde{\theta} - \mathrm{E}[\tilde{\theta}]\right)], \qquad \underline{\mathbf{R}} := f_R(\mathrm{E}[\tilde{\theta}]), \tag{14}$$

$$\psi = 2c\mathbf{r}^T (I - c\underline{\mathbf{R}})^{-1} \underline{\mathbf{R}}\mathbf{r} + \mathrm{Tr}\left[\mathbf{P} + \mathbf{b}\mathbf{b}^T\right] + (2\mathbf{b}^T + \mathbf{r}^T)(I - c\underline{\mathbf{R}})^{-1}\boldsymbol{\rho} \tag{12}$$

$$\begin{aligned}\omega(n) = {} & \mathbf{r}^T (I - c\underline{\mathbf{R}})^{-2} \left(I - 4c\underline{\mathbf{R}} + 2(c\underline{\mathbf{R}})^2 + 2(c\underline{\mathbf{R}})^{n+1}\right)\mathbf{r} - 2\mathbf{b}^T (I - c\underline{\mathbf{R}})^{-2} \left(I - (c\underline{\mathbf{R}})^n\right)\boldsymbol{\rho} \\ & + \mathbf{b}^T (I - c\underline{\mathbf{R}})^{-1} \left[I - (c\underline{\mathbf{R}})^n\right]\mathbf{r} - \mathbf{r}^T (I - c\underline{\mathbf{R}})^{-2} \left[I - (c\underline{\mathbf{R}})^n\right]\boldsymbol{\rho} - \| \left[(I - c\underline{\mathbf{R}})^{-1}(I - (c\underline{\mathbf{R}})^n)(c\underline{\mathbf{R}}\mathbf{r} + \boldsymbol{\rho})\right] \|_2^2\end{aligned}$$

and the scalars ψ, $\omega(n)$ are given in (12). □

IV. Simulation verification

In this section we empirically estimate the mean and covariance of the estimation error by conducting a Monte-Carlo simulation. When then compare the estimated mean with the theoretical predictions. We only consider the 2-D scenario with periodic trajectory so that the empirical result can be compared with the prediction of Theorem 2. All simulations are conducted in MATLAB©.

A. Straight-line trajectory

For the straight line case, we simulate a robot moving in a straight line on a plane with a constant velocity of $[0.2263, 0.2263]^{\mathrm{T}}\,\mathrm{m/s}$ and constant orientation. Two types of simulations are conducted. In the first type, which we call *simulated data*, noisy measurements of the rotation, i.e., $\hat{\theta}_{k-1,k}$ are generated as a Laplace distributed random variable using a pseudo-random number generator. Noisy measurements of the translations, i.e., ${}^k\hat{\mathbf{t}}_{k-1,k}$ were generated from noisy measurements of translation direction, which we call ${}^k\boldsymbol{\zeta}_{k-1,k}$, and translation magnitude, which we call $d_k \in \mathbb{R}^+$, as ${}^k\hat{\mathbf{t}}_{k-1,k} = \hat{d}_k\hat{\boldsymbol{\zeta}}_{k-1,k}$ ${}^k\hat{\mathbf{t}}_{k-1,k} = \hat{d}_k\,{}^k\hat{\boldsymbol{\zeta}}_{k-1,k}$, where $\hat{d}_k$ and ${}^k\hat{\boldsymbol{\zeta}}_{k-1,k}$ are noisy estimates of d_k and ${}^k\boldsymbol{\zeta}_{k-1,k}$, respectively. Note that ${}^k\boldsymbol{\zeta}_{k-1,k}$ is a 2-vector with unit norm. This is to simulate relative pose measurement with a monocular camera and IMU/wheel odometry. The camera provides only relative rotation and direction of translation, while the magnitude of translation is measured by another sensor, such as wheel encoders or inertial sensors.

In the second type of simulations, which we denote by *simulated camera*, the vision-based relative pose estimation sensor is simulated in a more realistic fashion by generating synthetic image data, from which relative rotation and direction of translation are estimated. The magnitude of translation measurements are generated as in the "simulated data" case.

Simulated data: At each time step k, a measurement of the relative orientation is constructed numerically as $\hat{\theta}_{k-1,k} = 0 + \tilde{\theta}_{k-1,k}$, where the orientation error $\tilde{\theta}_{k-1,k}$ is chosen to be a 0-mean Laplace distributed r.v. Recall that a Laplace distribution with μ mean and variance $2\lambda^2$ has the pdf $f(\tilde{\theta}) = \dfrac{1}{2\lambda}e^{-|\tilde{\theta}-\mu|/\lambda}$. The value of λ chosen is 3.6×10^{-3}, which best fits the orientation measurement error statistics generated by the synthetic monocular camera-based relative pose sensor, which is described in the sequel. The noisy measurement of translation direction ${}^k\hat{\boldsymbol{\zeta}}_{k-1,k}$ generated as

$${}^k\hat{\boldsymbol{\zeta}}_{k-1,k} = \begin{pmatrix}\cos\tilde{\phi}_{k-1,k} & -\sin\tilde{\phi}_{k-1,k} \\ \sin\tilde{\phi}_{k-1,k} & \cos\tilde{\phi}_{k-1,k}\end{pmatrix} {}^k\boldsymbol{\zeta}_{k-1,k}$$

where $\tilde{\phi}_{k-1,k}$ is a zero-mean Laplace random variable with variance 3.07×10^{-2} $3.07 \times 10^{-2}\,\mathrm{rad}^2$, and ${}^k\boldsymbol{\zeta}_{k-1,k} = \frac{1}{\sqrt{2}}[1,1]^T$ is the true translation direction. The magnitude of the translation is $d_k = 6.4 \times 10^{-2}$ m and its noisy measurement is generated as $\hat{d}_k = d_k + \tilde{d}_k$, where $\tilde{d}_k$ is a zero-mean Gaussian random variable with mean 0 variance $8.5467 \times 10^{-5}\ m^2$. These numbers are chosen to be consistent with those seen in an experiment with a wheeled robot described later in Section V. The values of the parameters that are needed to compute the predictions by Theorem 3, are determined by the choice of the measurement noise statistics, which turn out to be $\mathbf{b} = [-0.6842, -0.6842] \times 10^{-3}\,\mathrm{m}$, $\mathrm{Tr}\,[\mathrm{P}] = 1.2479 \times 10^{-4}\,\mathrm{m}^2$, and $c = 1 - 1.2873 \times 10^{-5}$.

The mean and covariance of the position estimation error at every time instant are empirically estimated by averaging over 76,600 Monte-Carlo simulations. Figure 2 presents the estimated mean and covariances, and the values predicted by Theorem 3. We see from the figure that the prediction from Theorem 3 matches estimates from Monte-Carlo simulations quite closely even for the large time intervals used in the simulations.

Simulated camera: We now simulate the scenario in which relative pose measurements are obtained by a calibrated monocular Prosilica EC 1020 camera and wheel odometers found on a Pioneer P3-DX. To simulate an estimate of the camera ego-motion between consecutive time steps, suppose between k and $k+1$, a set of 50 3-D points are randomly generated in the volume visible to the camera at time step k, with their coordinates represented in the reference frame attached to the camera at time step k. The points are then acted on by the true transformation from k to $k+1$ to find the corresponding coordinates in the reference frame attached to the camera at time step $k+1$, discarding any points falling outside the volume visible to the camera at that time step. Using a calibration matrix corresponding to the Prosilica EC 1020 camera, the points are projected into their corresponding image plane. This forms a set of correspondences analogous to the feature points extracted from actual image pairs. Each feature point is now corrupted by uniform noise with support lying in a 2×2 pixel square about the point. A RANSAC [13] assisted normalized 8-point algorithm [14] is used to estimate the rotation $\hat{R}$ and translation direction $\hat{\boldsymbol{\zeta}}$ between the two time steps from these point correspondences. The axis of rotation

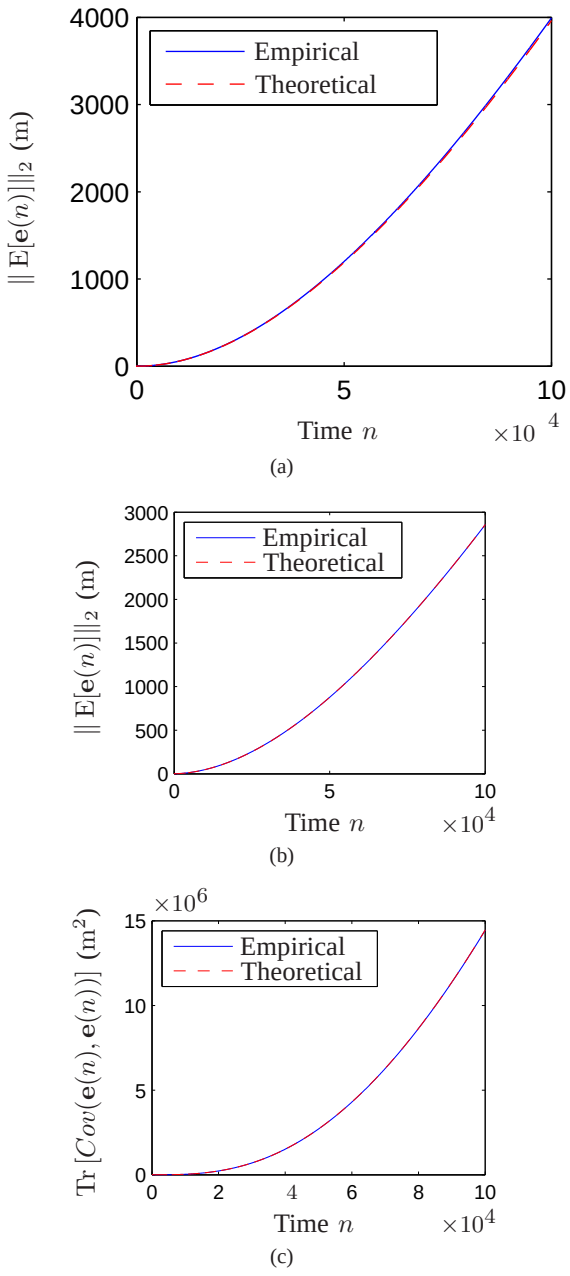

Fig. 2. 2-D scenario, straight line trajectory: Comparison of Theorem 3's predictions ("Theoretical") of bias and variance in position estimation error with those estimated from Monte-Carlo simulations ("Empirical"), for the "simulated data" case.

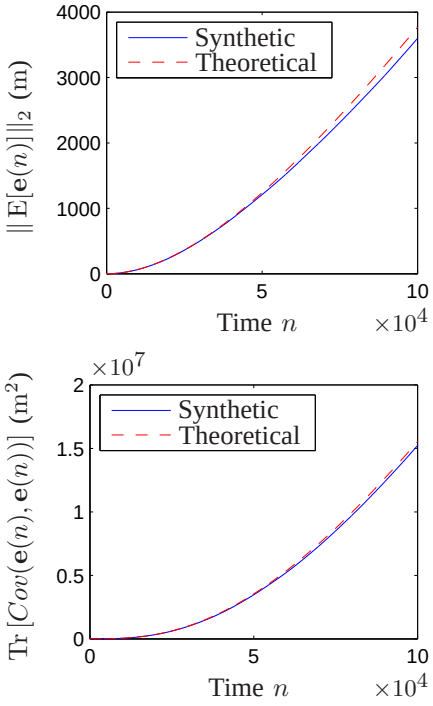

Fig. 3. 2-D scenario, straight line trajectory: Comparison of Theorem 3's predictions ("Theoretical") of bias and variance in position estimation error with those estimated from Monte-Carlo simulations ("Synthetic"), for the "simulated camera" case.

was then aligned with the normal to the plane of motion and the component of the translation vector in that direction was dropped to insure the motion estimates remained in the plane. The magnitude of translation $\hat{d}$ is generated as in the **Simulated Data** case. The values of the parameters that are needed to compute the predictions by Theorem 3 are estimated from Monte-Carlo experiments, in which the relative pose between two frames with a known pose is measured from synthetic image data, and by averaging over appropriate functions. The values are found to be $\mathbf{b} = [-0.5767, -0.5904] \times 10^{-5}\,\mathrm{m}$, $\mathrm{Tr}\,[\mathrm{P}] = 1.6382 \times 10^{-4}\,\mathrm{m}^2$, and $c = 1 - 2.1462 \times 10^{-5}$.

Figure 3 compares the predictions of bias and variance by Theorem 3 to those estimated from 1000 Monte-Carlo simulations. The number of Monte-Carlo simulations is smaller in the synthetic data case due to the prohibitively high cost of conducting these simulations. We see from Figure 3 that Theorem 3 accurately predicts the position estimation error computed from synthetic image data. The prediction toward the end of the simulation time is not as accurate as in the simulated data case, which is due to the smaller number of Monte-Carlo trials.

B. Periodic trajectory

For the periodic case, we simulate a robot moving on a circle with circumference of 4.11 m for approximately 5.5 hours, sampling the robot's relative pose every 0.2 seconds. The speed of the robot is approximately $0.32\,\mathrm{m/sec}$, so that it traverses the circle about 47 times before completing one period. This yields a periodic trajectory with period $p = 3020$. The trajectory is chosen to be close to that encountered in an experiments with a Pioneer P3-DX robot, which will be described in Section V.

For this simulation, noisy measurements of the rotation, i.e., $\hat{\theta}_{k-1,k}$ are generated as a Laplace distributed random variable using a pseudo-random number generator. Noisy measurements of the translations, i.e., ${}^k\hat{\mathbf{t}}_{k-1,k}$ were generated from noisy measurements of translation direction, which we call ${}^k\boldsymbol{\zeta}_{k-1,k}$, and translation magnitude, which we call $d_k \in \mathbb{R}^+$,

as ${}^k\hat{\mathbf{t}}_{k-1,k} = \hat{d}_k\, {}^k\hat{\boldsymbol{\zeta}}_{k-1,k}$, where $\hat{d}_k$ and ${}^k\hat{\boldsymbol{\zeta}}_{k-1,k}$ are noisy estimates of d_k and ${}^k\boldsymbol{\zeta}_{k-1,k}$, respectively. Note that ${}^k\boldsymbol{\zeta}_{k-1,k}$ is a 2-vector with unit norm. This is to simulate relative pose measurement with a monocular camera and IMU/wheel odometry. The camera provides only relative rotation and direction of translation, while the magnitude of translation is measured by another sensor, such as wheel encoders or inertial sensors.

At each time step k, a measurement of the relative orientation is constructed numerically as $\hat{\theta}_{k-1,k} = 6.8\times10^{-5} + \tilde{\theta}_{k-1,k}$, where the orientation error $\tilde{\theta}_{k-1,k}$ is chosen to be a 0-mean Laplace distributed r.v. Recall that a Laplace distribution with μ mean and variance $2\lambda^2$ has the pdf $f(\tilde{\theta}) = \dfrac{1}{2\lambda} e^{-|\tilde{\theta}-\mu|/\lambda}$. The value of λ chosen is 3.6×10^{-3}. The noisy measurement of translation direction ${}^k\hat{\boldsymbol{\zeta}}_{k-1,k}$ generated as

$$ {}^k\hat{\boldsymbol{\zeta}}_{k-1,k} = f_R(\tilde{\phi}_{k-1,k})\ {}^k\boldsymbol{\zeta}_{k-1,k} $$

where $\tilde{\phi}_{k-1,k}$ is a zero-mean Laplace random variable with variance $3.07 \times 10^{-2}\ \mathrm{rad}^2$, and ${}^k\boldsymbol{\zeta}_{k-1,k} = -\,[0.049, 0.999]^T$ is the true translation direction. The magnitude of the translation is $d_k = 6.4 \times 10^{-2}$ m and its noisy measurement is generated as $\hat{d}_k = d_k + \tilde{d}_k$, where $\tilde{d}_k$ is a zero-mean Gaussian random variable with mean 0 variance 8.5467×10^{-5} m^2. These numbers are again chosen to be consistent with the experiment described in Section V. The values of the parameters that are needed to compute the predictions by Theorem 2, are determined by the choice of the measurement noise statistics and are equal to $c = 1 - 1.29 \times 10^{-5}$ and $\rho_k = [0.047, 0.97]^T \times 10^{-3}$.

The mean and covariance of the position estimation error at every time instant are empirically estimated by averaging over 29,970 Monte-Carlo simulations. Figure 4 compares the predicted values from Theorem 2 with empirical estimates from the $29,970$ Monte-Carlo simulations. We see that the bias is quite accurately predicted by Theorem 2. The linear trend in variance observed from Monte Carlo simulations is consistent with prediction of Theorem 2.

V. Experimental verification

In this section we report results of experiments conducted with a wheeled Pioneer P3-DX robot that is equipped with a calibrated monocular Prosilica EC 1020 camera and wheel odometers. The images captured by the camera are used to estimate the relative rotation and direction of translation. The distance travelled estimated by the wheel odometers is fused with the direction of translation estimated from the camera to estimate the translation vector. The relative pose of the camera is measured every 0.2 seconds. An overhead camera is used to measure the true 2-D pose of the robot. Due to space constraints of the indoor test set-up, the trajectory of the robot was chosen to be an approximately circular one with radius 0.65 m and one rotation taking approximately 13 seconds (see Figure 5). The robot's trajectory is approximately periodic with period $p = 3020$ (i.e., 604 seconds).

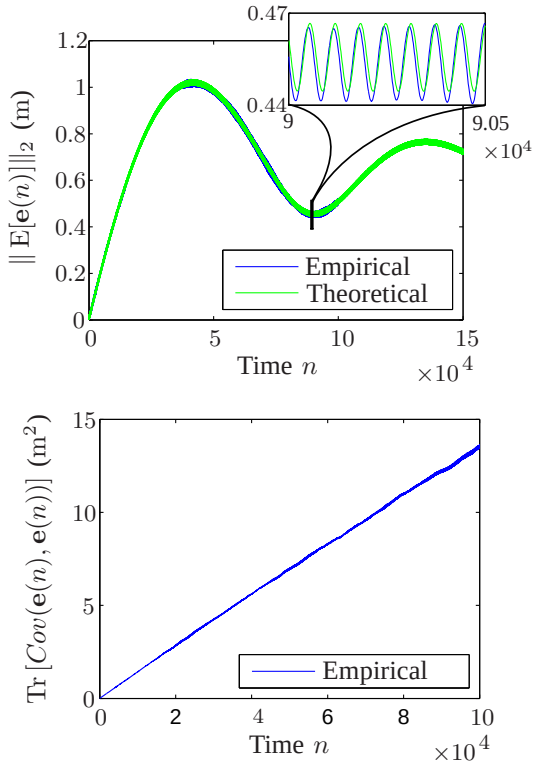

Fig. 4. 2-D scenario, periodic motion: Comparison of Theorem 2's predictions with estimates from Monte-Carlo simulations ("Empirical"). The legend "Theoretical" in (a) refers to the prediction from (10) in Theorem 2.

A. Test set-up

Figure 6(b) shows a schematic of the experimental set-up. The global coordinate frame is defined to coincide with the coordinate frame attached to an overhead camera viewing the plane of motion. That is, the origin of the global coordinate axes corresponds to the camera's focal point. The overhead camera is used to obtain the true pose of the robot. The robot's local coordinate frame was defined by a cube affixed to the top of the box. A grid consisting of six dots was placed atop the cube with a known geometry (see Figure 6(a)), which allows reconstruction of the full 3-D pose of the robot from the single monocular camera. Although some error between the true pose of the robot and that estimated from the overhead camera is inevitable, this error did not have any cumulative effect over time. Therefore we call the pose estimated from the overhead camera the "ground truth".

A KLT tracker [15] was used to track feature points across pairs of images, and a RANSAC-assisted normalized 8-point algorithm was used to estimate the relative rotation and direction of translation between every successive pairs of images. All estimation was performed off-line. Even with RANSAC, outliers in point-correspondences can cause large errors in the relative pose estimates. An ad-hoc "filter" was

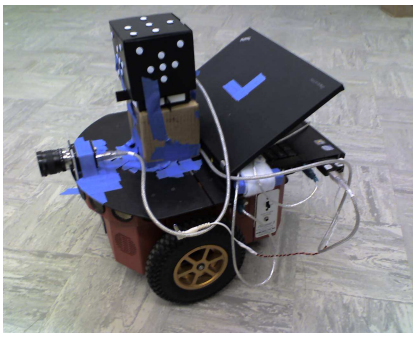

(a)

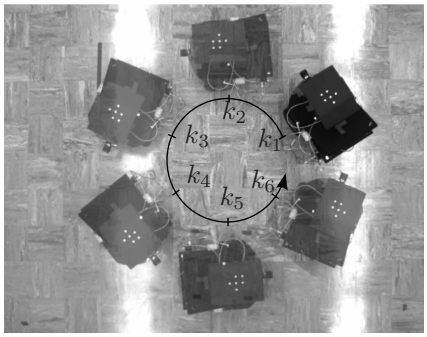

(b)

Fig. 5. (a)The robot used in the experiments, and (b) a few snapshots from the overhead camera showing the trajectory.

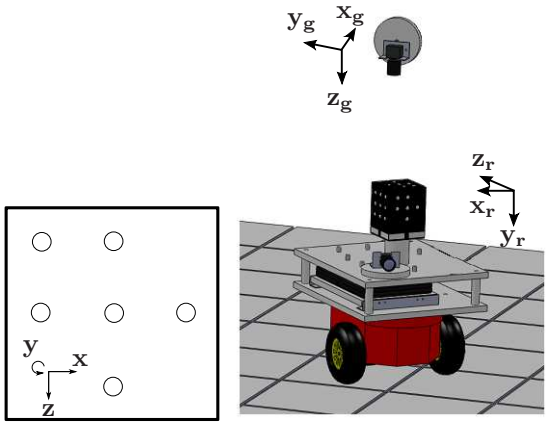

(a) Top view (b) Coordinate Axes

Fig. 6. Schematic of the test set-up.

implemented to reduce the effect of such errors as follows. If the estimated relative pose from the camera was deemed infeasible (which was determined by the known motion of the robot), the relative rotation and relative translation direction estimated in the previous time step was used as the estimate for the current time step. The relative translation between two time instants was estimated from the relative translation direction and the estimate of its magnitude, the latter being obtained from a wheel odometer. The relative poses so obtained were chained together to obtain an estimate of the global position and orientation of the robot at every time step, as described in Section II-A.

B. Test results

The position estimation error at each time step is computed by comparing the ground truth with the robot's position estimated from relative pose measurements. The bias and variance in the position estimation error at any given time step are determined by averaging over 17 experiments, where each experiment consists of the robot following its path for 1000 seconds (5000 time steps). The experimentally obtained bias and variance of position estimation error are shown in Figures 7(a) and 7(b). We see that the experimentally obtained results - especially the bias – closely follow those seen in simulations (cf. Figure 4(a),4(b)), which in turn are accurately predicted from the analysis. The experimentally obtained bias stays bounded, as Theorem 1 predicts. The variance also shows an on-average linear growth with time, which is consistent with Theorem 1. This provides additional confidence in our theoretical results. In addition, we note that while the theoretical predictions are for a dead-reckoning type position estimation algorithm, the algorithm used in the experiments was more akin to a kinematic-model based filter. Still the theoretical predictions match the experimental results rather well. This is expected, as discussed in Remark 1.

The discrepancies between the experimentally obtained bias and variance values and those obtained from simulations are due to the fact that our experiments and simulations differ in a number of ways. First, the experimental values are computed by averaging over only 17 experiments, whereas the simulation estimates are computed from at least 1000 Monte-Carlo simulations. The reason for this smaller number of experimental trials is the difficulty and time needed in performing these experiments. The smaller number of trials that were averaged over produced less accurate estimates. Second, the characteristics of the camera error could not be modeled in any of our simulations.

VI. Discussion and Summary

We examined the growth of error in position estimation from noisy relative pose measurements. We showed that both the bias and variance grows at most linearly with time or distance travelled. Although not presented here due to lack of space, when the robot loves in a straight line, both the bias and variance look super-linear for small values of time index n [12]. Only when the time n is sufficiently large that the linear asymptotic trend with n become clearly visible. This may be the reason for the super-linear error growth rate observed in certain experiments [4]. The precise growth rate depends on the trajectory of the robot. Exact formulas for the error growth rates are obtained for a special trajectory. Simulations, and experiments with a wheeled robot, were used to verify the results.

The results are established under the assumption that the errors in the relative orientation and position measurements are i.i.d. The results will still hold, though the analysis will be more involved, with the weaker assumption that $\|\,\mathrm{E}[\tilde{\mathbf{R}}_k]\| \leq \gamma < 1$ for some positive constant γ, instead

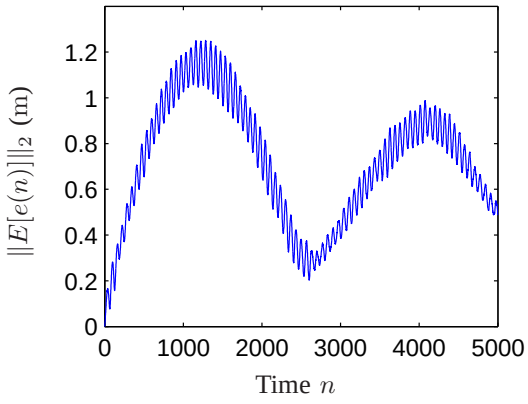

(a) Bias

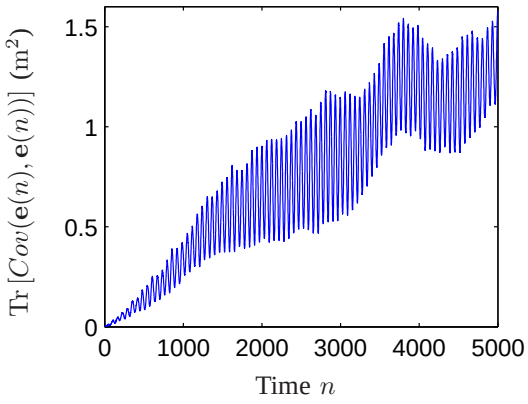

(b) Variance

Fig. 7. Bias and variance of position estimation error for a P3-DX robot (5000 time steps = 16.67 minutes).

of the rotation errors $\tilde{\mathbf{R}}_k$ being identically distributed. The independence assumption was made to simplify the analysis. Experimental results closely match the theoretical predictions made, indicating the results may not be sensitive to this assumption. We emphasize that the rotation and translation measurement errors are not assumed to be small for any of the results.

The error growth trends are ultimately due to the fact that $\| \mathrm{E}[\mathbf{R}_k] \| < 1$, which causes the position estimates to converge to a point by causing a geometric decay, on average, of the magnitude of the relative translation estimate when expressed in the global coordinate. In principle, knowledge of the measurement error statistics can be used to compensate for this decay. This is a subject of ongoing work.

References

[1] T. Oskiper, Z. Zhu, S. Samarasekera, and R. Kumar, "Visual odometry system using multiple stereo cameras and inertial measurement unit," in *IEEE Conference on Computer Vision and Pattern Recognition (CVPR '07)*, 17-22 June 2007, pp. 1–8.

[2] O. Mezentsev and G. Lachapelle, "Pedestrian dead reckoning - a solution to navigation in GPS signal degraded areas?" *Geomatica*, vol. 59, no. 2, pp. 175–182, 2005.

[3] R. C. Smith and P. Cheeseman, "On the representation and estimation of spatial uncertainty," *International Journal of Robotics Research*, vol. 5, no. 4, pp. 56–68, 1986.

[4] C. F. Olson, L. H. Matthies, M. Schoppers, and M. W. Maimone, "Rover navigation using stereo ego-motion," *Robotics and Autonomous Systems*, vol. 43, no. 4, pp. 215–229, June 2003.

[5] S. Roumeliotis and I. Rekleitis, "Analysis of multirobot localization uncertainty propagation," in *IEEE/RSJ International Conference on Intelligent Robots and Systems*, vol. 2, 2003, pp. 1763 – 1770.

[6] S. Su and C. S. G. Lee, "Manipulation and propagation of uncertainty and verification of applicability of actions in assembly tasks," *IEEE Transactions on Systems, Man, and Cybernetics*, vol. 22, no. 6, pp. 1376–1389, 1982.

[7] Y. Wang and G. S. Chirikjian, "Error propagation on the euclidean group with applications to manipulator kinematics," *IEEE Transactions on Robotics*, vol. VOL. 22, no. 4, pp. 1–12, Jul 2006.

[8] Y. Wang and G. Chirikjian, "Nonparametric-second order theory of error propagation on motion groups," *International Journal of Robotics Research*, vol. 27, no. 11-12, pp. 1258–1273, 2008.

[9] P. Smith, T. Drummond, and K. Roussopoulos, "Computing MAP trajectories by representing, propagating and combining pdfs over groups," in *IEEE International Conference on Computer Vision*, vol. 2, 2003, pp. 1275–1282.

[10] J. Kwon, M. Choi, F. Park, and C. Chun, "Particle filtering on the euclidean group: framework and applications," *Robotica*, vol. 25, pp. 725–737, 2007.

[11] R. M. Murray, Z. Li, and S. S. Sastry, *A Mathematical Introduction to Robotic Manipulation*, 1994, ch. 2.2.

[12] J. Knuth and P. Barooah, "Error scaling in position estimation from noisy relative pose measurements," University of Florida, Tech. Rep., March 2011. [Online]. Available: http://plaza.ufl.edu/knuth/Publications/

[13] M. Fischler and L. Bolles, "Random sample consensus: A paradigm for model fitting with applications to image analysis and automated cartography," *Communications of the ACM*, vol. 24, pp. 381–385, 1981.

[14] R. Hartley and A. Zisserman, *Multiple View Geometry in Computer Vision*. Cambridge University Press, 2004.

[15] C. Tomasi and T. Kanade, "Detection and tracking of point features," Carnegie Mellon University, Tech. Rep., April 1991.

Appendix

The following technical results will be needed for the remaining proofs.

Proposition 1: Let $\mathbf{R}$ be a random rotation matrix with distribution defined over $SO(d)$, $d \geq 2$ and $\mathrm{E}[\mathbf{R}]$ is a $d \times d$ matrix whose i,j-th entry is the expected value of the i,-th entry of $\mathbf{R}$. We have $\| \mathrm{E}[\mathbf{R}] \| \leq 1$, and the inequality is strict if the distribution of $\mathbf{R}$ is not degenerate (meaning it is not concentrated at one point). □

Proof of Proposition 1: Let $\mathbf{y}$ be a d-dimensional random vector. Since $Cov(\mathbf{y}, \mathbf{y}) = \mathrm{E}[\mathbf{y}\mathbf{y}^T] - \mathrm{E}[\mathbf{y}]\,\mathrm{E}[\mathbf{y}]^T$, we have upon taking the trace of both sides

$$\| \mathrm{E}[\mathbf{y}] \|^2 = \mathrm{E}[\|\mathbf{y}\|^2] - \mathrm{Tr}\,[Cov(\mathbf{y}, \mathbf{y})] \leq \mathrm{E}[\|\mathbf{y}\|^2],$$

since $\mathrm{Tr}\,[Cov(\mathbf{y}, \mathbf{y})] \geq 0$. Moreover equality in the above inequality holds if and only if the variance of each of the components of $\mathbf{y}$ is 0, that is $\mathbf{y}$ is a constant vector a.s. We now apply this result to the random vector $\mathbf{y} := \mathbf{R}x$, where x is a deterministic d-dimensional vector while $\mathbf{R}$ is a random rotation matrix. Since $\mathbf{y}$ is degenerate if only if $\mathbf{R}$ is, we have

$$\| \mathrm{E}[\mathbf{R}]x \|^2 < \mathrm{E}[\|\mathbf{R}x\|^2] = \mathrm{E}[\|x\|^2]$$

since rotation doesn't change the 2-norm of a vector. This proves that $\| \mathrm{E}[\mathbf{R}] \| < 1$ as long as $\mathbf{R}$ is not degenerate. ■

Proposition 2: If X_i is a sequence of random vectors such that $\mathrm{E}[X_i^T X_j] \leq \overline{\alpha_0}\gamma^{|i-j|}$, where $|\gamma| < 1$ and $\overline{\alpha_0}$ is an arbitrary constant, then $\mathrm{E}[(\sum_{i=1}^n X_i)^T (\sum_{i=1}^n X_i)] = O(n)$. If in addition $\underline{\alpha_0}\gamma^{|i-j|} \leq \mathrm{E}[X_i^T X_j]$ for $i \neq j$ and $0 < \beta_0 \leq$

$\mathrm{E}[X_i^T X_i]$, where $\underline{\alpha_0}, \underline{\beta_0}$ are constants such that $\underline{\beta_0} > 2\frac{|\underline{\alpha_0}|}{1-|\gamma|}$, then $\mathrm{E}[(\sum_{i=1}^n X_i)^T(\sum_{i=1}^n X_i)] = \Theta(n)$.

Proof of Proposition 2: Expanding the sum, we obtain

$$\mathrm{E}[(\sum_{i=1}^n X_i)^T(\sum_{i=1}^n X_i)] = \sum_{i=1}^n T_i, \tag{15}$$

where

$$T_i := \sum_{j=1}^n \mathrm{E}[X_i^T X_j]. \tag{16}$$

It follows from (16) and the hypothesis that

$$\begin{aligned} T_i &\le \overline{\alpha_0}(\gamma^{i-1} + \gamma^{i-2} + \cdots + \gamma + 1 + \gamma + \cdots + \gamma^{n-i}) \\ &= \overline{\alpha_0}(-1 + \sum_{k=0}^{i-1}\gamma^k + \sum_{k=0}^{n-i}\gamma^k) \le \overline{\alpha_0}(-1 + \sum_{k=0}^{\infty}|\gamma|^k + \sum_{k=0}^{\infty}|\gamma|^k) \\ &= \overline{\alpha_0}(-1 + \frac{1}{1-|\gamma|} + \frac{1}{1-|\gamma|}) = \overline{\alpha_0}\frac{1+|\gamma|}{1-|\gamma|}, \end{aligned}$$

where the second inequality follows from $|\gamma| < 1$. This shows that $T_i = O(1)$. It now follows from (15) that $\mathrm{E}[(\sum_{i=1}^n X_i)^T(\sum_{i=1}^n X_i)] = O(n)$. This proves the first statement.

When the additional hypothesis holds, we have

$$\begin{aligned} T_i &\ge \underline{\alpha_0}(\gamma^{i-1} + \gamma^{i-2} + \cdots + \gamma) + \underline{\beta_0} + \underline{\alpha_0}(\gamma + \cdots + \gamma^{n-i}) \\ &\ge -2|\underline{\alpha_0}|\sum_{k=0}^{\infty}|\gamma|^k + \underline{\beta_0} = \underline{\beta_0} - 2\frac{|\underline{\alpha_0}|}{1-|\gamma|} =: \ell_0 > 0 \end{aligned}$$

It follows from (15) that $\mathrm{E}[(\sum_{i=1}^n X_i)^T(\sum_{i=1}^n X_i)] \ge n\ell_0 = \Omega(n)$. Combining the asymptotic lower and upper bounds, we get $\mathrm{E}[(\sum_{i=1}^n X_i)^T(\sum_{i=1}^n X_i)] = \Theta(n)$. ∎

Proof of Lemma 1: It follows from (4) that

$$\mathrm{E}[{}^0\hat{\mathbf{t}}_{0,n}] = \sum_{k=1}^n \mathrm{E}[{}^0\hat{\mathbf{t}}_{k,k+1}] \tag{17}$$

From (2)-(3), and using commutativity of 2-D rotation matrices, we get

$$\begin{aligned} {}^0\hat{\mathbf{t}}_{k,k+1} &= {}_{k+1}^{0}\mathbf{R}\,{}_{1}^{0}\tilde{\mathbf{R}}\cdots{}_{k+1}^{k}\tilde{\mathbf{R}}\left({}^{k+1}\mathbf{t}_{k,k+1} + {}^{k+1}\tilde{\mathbf{t}}_{k,k+1}\right) \\ \Rightarrow \mathrm{E}[{}^0\hat{\mathbf{t}}_{k,k+1}] &= {}_{k+1}^{0}\mathbf{R}\left(\bar{\mathbf{R}}^{k+1}\ {}^{k+1}\mathbf{t}_{k,k+1} + \bar{\mathbf{R}}^k\ \boldsymbol{\rho}_{k+1}\right) \end{aligned}$$

where the second equality follows from the assumption that the orientation measurement errors are i.i.d. Since a rotation does not change the 2-norm of a vector,

$$\begin{aligned} \|\,\mathrm{E}[{}^0\hat{\mathbf{t}}_{k,k+1}]\| &= \|\left(\bar{\mathbf{R}}^{k+1}\ {}^{k+1}\mathbf{t}_{k,k+1} + \bar{\mathbf{R}}^k\boldsymbol{\rho}_k\right)\| \\ &\le \|\bar{\mathbf{R}}^k\|\left(\|\bar{\mathbf{R}}\|\|{}^{k+1}\mathbf{t}_{k,k+1}\| + \|\boldsymbol{\rho}_{k+1}\|\right) \end{aligned}$$

where the inequality follows from applying triangle inequality and using sub-multiplicative property of induced norms. Since $\|\bar{\mathbf{R}}^k\| \le \|\bar{\mathbf{R}}\|^k$, we obtain upon using Proposition 1 and the definition $\gamma = \|\bar{\mathbf{R}}\|$ that $\|\,\mathrm{E}[{}^0\hat{\mathbf{t}}_{k,k+1}]\| \le \gamma^k a$, where $a := \sup_k(\|\bar{\mathbf{R}}\|\|{}^{k+1}\mathbf{t}_{k,k+1}\| + \|\boldsymbol{\rho}_{k+1}\|) \le \gamma\tau + \beta$. Note that $0 < \gamma < 1$. Applying triangle inequality to (17), we get

$$\|\,\mathrm{E}[{}^0\hat{\mathbf{t}}_{0,n}]\| \le \sum_{k=0}^{n-1}\|\,\mathrm{E}[{}^0\hat{\mathbf{t}}_{k,k+1}]\| \quad \le a\sum_{k=0}^{n-1}\gamma^k \le a\frac{1}{1-\gamma},$$

since $0 < \gamma < 1$. This proves the result about the mean.
The proof for the second moment result relies on Proposition 2. For $i \le j$,

$$\begin{aligned} ({}^0\hat{\mathbf{t}}_{i,i+1})^T\,{}^0\hat{\mathbf{t}}_{j,j+1} &= ({}^{i+1}\hat{\mathbf{t}}_{i,i+1}\,{}_{i+1}^{0}\hat{\mathbf{R}})^T\ {}_{j+1}^{0}\hat{\mathbf{R}}^{j+1}\hat{\mathbf{t}}_{j,j+1} \\ &= ({}^{i+1}\hat{\mathbf{t}}_{i,i+1})^T\ {}_{j+1}^{i+1}\hat{\mathbf{R}}\ {}^{j+1}\hat{\mathbf{t}}_{j,j+1} \\ &= V_1 + V_2 + V_3 + V_4, \end{aligned}$$

where

$$\begin{aligned} V_1 &:= ({}^{i+1}\mathbf{t}_{i,i+1})^T\ {}_{j+1}^{i+1}\hat{\mathbf{R}}\ {}^{j+1}\mathbf{t}_{j,j+1} \\ V_2 &:= ({}^{i+1}\tilde{\mathbf{t}}_{i,i+1})^T\ {}_{j+1}^{i+1}\hat{\mathbf{R}}\ {}^{j+1}\mathbf{t}_{j,j+1} \\ V_3 &:= ({}^{i+1}\mathbf{t}_{i,i+1})^T\ {}_{j+1}^{i+1}\hat{\mathbf{R}}\ {}^{j+1}\tilde{\mathbf{t}}_{j,j+1} \\ V_4 &:= ({}^{i+1}\tilde{\mathbf{t}}_{i,i+1})^T\ {}_{j+1}^{i+1}\hat{\mathbf{R}}\ {}^{j+1}\tilde{\mathbf{t}}_{j,j+1}. \end{aligned}$$

We now evaluate the expected values of these four terms. By using the Independence of the orientation measurement errors and commutativity of 2-D rotation matrices, we get $\mathrm{E}[{}_{j+1}^{i+1}\hat{\mathbf{R}}] = {}_{j+1}^{i+1}\mathbf{R}\,\bar{\mathbf{R}}^{j-i}$. Therefore,

$$\begin{aligned} \mathrm{E}[V_1] &= ({}^{i+1}\mathbf{t}_{i,i+1})^T\ {}_{j+1}^{i+1}\mathbf{R}\,\bar{\mathbf{R}}^{j-i}\ {}^{j+1}\mathbf{t}_{j,j+1} \\ \Rightarrow |\,\mathrm{E}[V_1]| &\le \|^{i+1}\mathbf{t}_{i,i+1}\|\|\bar{\mathbf{R}}^{j-i}\ {}^{j+1}\mathbf{t}_{j,j+1}\| \\ &\le \|\bar{\mathbf{R}}^{j-i}\|\|^{i+1}\mathbf{t}_{i,i+1}\|\|^{j+1}\mathbf{t}_{j,j+1}\| \le \gamma^{j-i}\tau^2, \end{aligned}$$

where the first inequality uses the fact that ${}_{j+1}^{i+1}\mathbf{R}$, being a rotation matrix, does not change the 2-norm. For V_2, since ${}^{i+1}\tilde{\mathbf{t}}_{i,i+1}$ is statistically dependent only on ${}_{i}^{i+1}\tilde{\mathbf{R}}$ and not on ${}_{i+1}^{i+2}\tilde{\mathbf{R}}, \ldots, {}_{j}^{j+1}\tilde{\mathbf{R}}$, it is also independent of ${}_{j+1}^{i+1}\hat{\mathbf{R}}$. Hence,

$$\begin{aligned} \mathrm{E}[V_2] &= \mathbf{b}_i^T\ {}_{j+1}^{i+1}\mathbf{R}\,\bar{\mathbf{R}}^{j-i}\ {}^{j+1}\mathbf{t}_{j,j+1} \\ \Rightarrow |\,\mathrm{E}[V_2]| &\le \gamma^{j-i}\ b\tau \end{aligned}$$

Similarly, we have, for $(i < j)$,

$$\begin{aligned} \mathrm{E}[V_3] &= ({}^{i}\mathbf{t}_{i+1,i+1})^T\ {}_{j+1}^{i+1}\mathbf{R}\,\bar{\mathbf{R}}^{j-i-1}\ \boldsymbol{\rho}_{j+1} \\ \Rightarrow |\,\mathrm{E}[V_3]| &\le \gamma^{j-i}\frac{1}{\gamma}\tau\rho. \end{aligned}$$

and for $i = j$, $|\,\mathrm{E}[V_3]| \le \tau b$. For V_4, when $i < j$, we have

$$V_4 = ({}^{i+1}\tilde{\mathbf{t}}_{i,i+1})^T\ {}_{j+1}^{i+1}\mathbf{R}\ {}_{i+2}^{i+1}\tilde{\mathbf{R}}\cdots{}_{j+1}^{j}\tilde{\mathbf{R}}\ {}^{j+1}\tilde{\mathbf{t}}_{j,j+1},$$

and using Assumption 2 about ${}^{j+1}\tilde{\mathbf{t}}_{j,j+1}$'s, we obtain

$$\begin{aligned} \mathrm{E}[V_4] &= \mathbf{b}_i^T\,{}_{j+1}^{i+1}\mathbf{R}\,\bar{\mathbf{R}}^{j-i-1}\boldsymbol{\rho}_{j+1} \\ \Rightarrow |\,\mathrm{E}[V_4]| &\le \gamma^{j-i}\frac{1}{\gamma}b\rho. \end{aligned}$$

For $i = j$, we have $V_4 = ({}^{j+1}\tilde{\mathbf{t}}_{j,j+1})^T\ {}^{j+1}\tilde{\mathbf{t}}_{j,j+1}$, which implies $\mathrm{E}[V_4] = \mathrm{Tr}\,[P_{j+1}] + \mathbf{b}_{j+1}^T\mathbf{b}_{j+1}$, by definition. Therefore,

$$0 < \underline{p} \le \mathrm{E}[V_4] \le \overline{p} + b^2. \quad (i = j).$$

Combining all four terms, we get,

$$\underline{\alpha_0}\gamma^{j-i} \leq \mathrm{E}[({}^0\hat{\mathbf{t}}_{i,i+1})^T {}^0\hat{\mathbf{t}}_{j,j+1}] \leq \alpha_0\gamma^{j-i}, \quad (i<j)$$
$$\underline{\beta_0} \leq \mathrm{E}[({}^0\hat{\mathbf{t}}_{i,i+1})^T {}^0\hat{\mathbf{t}}_{i,i+1}] \leq \beta_0,$$

where $\underline{\alpha_0} := -(\tau^2+\tau b+\frac{1}{\gamma}\tau\rho+\frac{1}{\gamma}b\rho)$, $\alpha_0 := \tau^2+\tau b+\frac{1}{\gamma}\tau\rho+\frac{1}{\gamma}b\rho$, and $\underline{\beta_0} := \underline{p}-(\tau^2+2\tau b)$, $\beta_0 := \tau^2+2\tau b+\overline{p}+b^2$. Note that in case $\underline{\beta_0}$ is negative, it is a poor lower lower bound since $({}^0\hat{\mathbf{t}}_{i,i+1})^T {}^0\hat{\mathbf{t}}_{i,i+1} > 0$. Repeating these arguments for $i \geq j$ and combining, we find that

$$\underline{\alpha_0}\gamma^{|i-j|} \leq \mathrm{E}[({}^0\hat{\mathbf{t}}_{i,i+1})^T {}^0\hat{\mathbf{t}}_{j,j+1}] \leq \overline{\alpha_0}\gamma^{|i-j|}. \quad (i\neq j)$$
$$\max\{0,\underline{\beta_0}\} \leq \mathrm{E}[({}^0\hat{\mathbf{t}}_{i,i+1})^T {}^0\hat{\mathbf{t}}_{i,i+1}] \leq \overline{\alpha_0}.$$

where $\overline{\alpha_0} := \max\{\alpha_0,\beta_0\}$. Now call $X_i := {}^0\hat{\mathbf{t}}_{i,i+1}$, so that ${}^0\hat{\mathbf{t}}_{0,n} = \sum_{i=0}^{n-1} X_i$. Hence, $\mathrm{E}[({}^0\hat{\mathbf{t}}_{0,n})^T {}^0\hat{\mathbf{t}}_{0,n}] = \mathrm{E}[(\sum_{i=0}^{n-1} X_i)^T(\sum_{j=0}^{n-1} X_j)]$. It now follows from Proposition 2 that $\mathrm{E}[({}^0\hat{\mathbf{t}}_{0,n})^T {}^0\hat{\mathbf{t}}_{0,n}]$ is $O(n)$, and is $\Theta(n)$ if $\underline{\beta_0} > 2\frac{|\underline{\alpha_0}|}{1-\gamma}$. Since $|\underline{\alpha_0}| = \tau^2+\tau b+\tau\rho$, the condition $\underline{\beta_0} > 2\frac{|\underline{\alpha_0}|}{1-\gamma}$ is equivalent to $\underline{p} > 2b\tau+\tau^2+2\dfrac{(\tau+\rho/\gamma)(\tau+b)}{1-\gamma}$, which proves the result. ∎

Proof of Theorem 2: Define a new random variable, $\delta\tilde{\theta}_{k-1,k} := \tilde{\theta}_{k-1,k} - \mathrm{E}[\tilde{\theta}_{k-1,k}]$. The sequence $\{\delta\tilde{\theta}_{k-1,k}\}_{k=0}^{\infty}$ are then i.i.d. and the marginal density of $\delta\tilde{\theta}_{k-1,k}$ is symmetric about the origin for each k. We define the corresponding rotation matrices ${}^i_j\tilde{\mathbf{R}}_\delta := f_R(\delta\tilde{\theta}_{i,j})$. Utilizing the commutative property of rotations in 2-D, we have the following relation

$${}^i_j\tilde{\mathbf{R}} = \left(\underline{\mathbf{R}}^{j-i}\right) {}^i_j\tilde{\mathbf{R}}_\delta \tag{18}$$

To examine the bias, we first re-write the position estimate ${}^0\hat{\mathbf{t}}_{0,n}$ as

$$\begin{aligned} {}^0\hat{\mathbf{t}}_{0,n} &= \sum_{i=0}^{n} {}^0\hat{\mathbf{t}}_{i,i+1} = \sum_{k=0}^{\eta-1}\left(\sum_{m=1}^{p} {}^0\hat{\mathbf{t}}_{kp+m-1,kp+m}\right) \\ &\quad + \sum_{j=1}^{q} {}^0\hat{\mathbf{t}}_{\eta p+j-1,\eta p+j}, \end{aligned} \tag{19}$$

where the first term is sum is over all time steps up to the end of the last (η-th) period and the second term for the time steps after that. For any $0 \leq m < p$, we have

$$\begin{aligned} {}^0\hat{\mathbf{t}}_{kp+m-1,kp+m} &= {}^0_{kp+m}\hat{\mathbf{R}}\ {}^{kp+m}\hat{\mathbf{t}}_{kp+m-1,kp+m} \\ &= {}^0_m\mathbf{R}\ {}^0_{kp+m}\tilde{\mathbf{R}}({}^m\mathbf{t}_{m-1,m} + {}^{kp+m}\tilde{\mathbf{t}}_{kp+m-1,kp+m}), \end{aligned}$$

where apart from $\hat{R} = R\tilde{R}$, we have used the periodic nature of the trajectory that leads to ${}^0_{kp+m}\mathbf{R} = {}^0_m\mathbf{R}$ and ${}^{kp+m}\mathbf{t}_{kp+m-1,kp+m} = {}^m\mathbf{t}_{m-1,m}$. Taking expectation and using (18), we obtain

$$\mathrm{E}[{}^0\hat{\mathbf{t}}_{kp+m-1,kp+m}] = {}^0_m\mathbf{R}(c\underline{\mathbf{R}})^{kp+m-1}(c\underline{\mathbf{R}}^m\mathbf{t}_{m-1,m} + \boldsymbol{\rho}_m)$$

This expression is used to evaluate $\mathrm{E}[{}^0\mathbf{t}_{0,n}]$ by taking expectation of the right hand side of (19). After grouping terms, we obtain

$$\mathrm{E}[{}^0\mathbf{t}_{0,n}] = \left(\sum_{k=0}^{\eta-1}(c\underline{\mathbf{R}})^{kp}\omega(p)\right) + (c\underline{\mathbf{R}})^{\eta p}\omega(q) \tag{20}$$

Finally, noting that the periodic motions implies

$${}^0\mathbf{t}_{0,n} = {}^0\mathbf{t}_{0,\eta p+q} = {}^0\mathbf{t}_{0,q} \tag{21}$$

and utilizing (5) we have

$$\mathrm{E}[\mathbf{e}(n)] = {}^0\mathbf{t}_{0,q} - \sum_{k=0}^{\eta-1}(c\underline{\mathbf{R}})^{kp}\, w(p) - (c\underline{\mathbf{R}})^{\eta p}w(q).$$

By replacing the summation we arrive at (10). ∎

Proof of Theorem 3: Define a new random variable, $\delta\tilde{\theta}_{k-1,k} := \tilde{\theta}_{k-1,k} - \mathrm{E}[\tilde{\theta}_{k-1,k}]$. Then $\{\delta\tilde{\theta}_{k-1,k}\}_{k=0}^{\infty}$ is an i.i.d. sequence and the marginal density of $\delta\tilde{\theta}_{k-1,k}$ is symmetric about 0. We define the corresponding rotation matrices ${}^i_j\tilde{\mathbf{R}}_\delta := f_R(\delta\tilde{\theta}_{i,j})$. Utilizing the commutative property of 2-D rotation matrices, we have ${}^i_j\tilde{\mathbf{R}} = \left(\underline{\mathbf{R}}^{j-i}\right) {}^i_j\tilde{\mathbf{R}}_\delta$. It then follows from (5) that

$$\mathbf{e}(n) = n\mathbf{r} - {}^0\hat{\mathbf{t}}_{0,n}$$

and from (4), (3), and (2) that

$${}^0\hat{\mathbf{t}}_{0,n} = \sum_{k=1}^{n}\left(\prod_{i=1}^{k}\underline{\mathbf{R}}^{i-1}\,{}^{i-1}_i\tilde{\mathbf{R}}_\delta\right)\left(\mathbf{r} + {}^k\tilde{\mathbf{t}}_{k-1,k}\right),$$

where we have used the fact that ${}^{i-1}_i\hat{\mathbf{R}} = {}^{i-1}_i\mathbf{R}\,{}^{i-1}_i\tilde{\mathbf{R}} = \underline{\mathbf{R}}^{i-1}\,{}^{i-1}_i\tilde{\mathbf{R}}_\delta$ since ${}^{i-1}_i\mathbf{R} = I$ due to the nature of the trajectory. We define two new random variables

$$\mathbf{f}_n := \sum_{k=1}^{n}\left(\prod_{i=1}^{k}\underline{\mathbf{R}}^{i-1}\,{}^{i-1}_i\tilde{\mathbf{R}}_\delta\right)\mathbf{r}$$
$$\mathbf{g}_n := \sum_{k=1}^{n}\left(\prod_{i=1}^{k}\underline{\mathbf{R}}^{i-1}\,{}^{i-1}_i\tilde{\mathbf{R}}_\delta\right)\,{}^k\tilde{\mathbf{t}}_{k-1,k},$$

so that

$${}^0\hat{\mathbf{t}}_{0,n} = \mathbf{f}_n + \mathbf{g}_n. \tag{22}$$

By the i.i.d. assumption on the sequence $\{\tilde{\theta}_{k-1,k}\}_k$, the sequence $\{{}^{k-1}_k\tilde{\mathbf{R}}_\delta\}_k$ is also i.i.d., so that

$$\mathrm{E}[{}^i_j\tilde{\mathbf{R}}_\delta] = \mathrm{E}[\prod_{k=i+1}^{k}{}^{k-1}_k\tilde{\mathbf{R}}_\delta] = \prod_{k=i-1}^{j}\mathrm{E}[{}^{k-1}_k\tilde{\mathbf{R}}_\delta] = c^{j-i}I, \tag{23}$$

where we have used the fact that $\mathrm{E}[\sin\delta\tilde{\theta}_{i-1,i}] = 0$, which follows from assumption that the distribution of θ is symmetric around 0. It is then straightforward to show that

$$\mathrm{E}[\mathbf{f}_n] = \sum_{k=1}^{n}(c\underline{\mathbf{R}})^k\,\mathbf{r} = (I-c\underline{\mathbf{R}})^{-1}\,(I-(c\underline{\mathbf{R}})^n)\,c\underline{\mathbf{R}}\mathbf{r}$$
$$\mathrm{E}[\mathbf{g}_n] = \sum_{k=0}^{n-1}(c\underline{\mathbf{R}})^k\,\boldsymbol{\rho} = (I-c\underline{\mathbf{R}})^{-1}\,(I-(c\underline{\mathbf{R}})^n)\,\boldsymbol{\rho}$$

The expected value $\mathbf{e}(n)$ is now

$$\mathrm{E}[\mathbf{e}(n)] = n\,\mathbf{r} - (I - c\underline{\mathbf{R}})^{-1}\,(I - (c\underline{\mathbf{R}})^n)\,(c\underline{\mathbf{R}}\mathbf{r} + \boldsymbol{\rho}) \quad (24)$$

which proves the first equality in (13).

For the variance, it follows from (22) that

$$\begin{aligned}\mathrm{Tr}\,[Cov(\mathbf{e}(n),\mathbf{e}(n))] &= \mathrm{Tr}\left[Cov({}^0\hat{\mathbf{t}}_{0,n},\,{}^0\hat{\mathbf{t}}_{0,n})\right] \\ &= \mathrm{E}[\mathbf{f}_n^T\mathbf{f}_n] + \mathrm{E}[\mathbf{g}_n^T\mathbf{g}_n] + 2\,\mathrm{E}[\mathbf{f}_n^T\mathbf{g}_n] \\ &\quad - \mathrm{E}[{}^0\hat{\mathbf{t}}_{0,n}]^T\,\mathrm{E}[{}^0\hat{\mathbf{t}}_{0,n}]. \qquad (25)\end{aligned}$$

$$\begin{aligned}\mathrm{E}[\mathbf{f}_n^T\mathbf{f}_n] &= \mathbf{r}^T\,\mathrm{E}\left[\sum_{i=1}^{n}\left(\prod_{j=1}^{i}\underline{\mathbf{R}}^{\,j-1}\,{}_j\tilde{\mathbf{R}}_\delta\right)^T\sum_{k=1}^{n}\left(\prod_{\ell=1}^{k}\underline{\mathbf{R}}^{\,\ell-1}\,{}_\ell\tilde{\mathbf{R}}_\delta\right)\right]\mathbf{r} \\ &= \mathbf{r}^T\Big[\left(I + c\underline{\mathbf{R}}^T + \cdots + (c\underline{\mathbf{R}}^T)^{n-1}\right) \\ &\quad + \left(c\underline{\mathbf{R}} + I + c\underline{\mathbf{R}}^T + \cdots + (c\underline{\mathbf{R}}^T)^{n-2}\right) \\ &\quad \cdots + \left((c\underline{\mathbf{R}})^{n-1} + \cdots + I\right)\Big]\mathbf{r}\end{aligned}$$

where we have used the independence of the sequence $\{{}^{k-1}_{\ k}\tilde{\mathbf{R}}_\delta\}_k$ and the fact that ${}^{k-1}_{\ k}\tilde{\mathbf{R}}_\delta\,{}^{k-1}_{\ k}\tilde{\mathbf{R}}_\delta^T = I = \underline{\mathbf{R}}\mathbf{R}^T$. The expression above simplifies to

$$\begin{aligned}\mathrm{E}[\mathbf{f}_n^T\mathbf{f}_n] &= \mathbf{r}^T\left[nI + 2\sum_{k=1}^{n-1}(n-k)\,(c\underline{\mathbf{R}})^k\right]\mathbf{r} = \mathbf{r}^T\,(I - c\underline{\mathbf{R}})^{-2} \\ &\quad \times\left(I + 2(n-2)c\underline{\mathbf{R}} - 2(n-1)\,(c\underline{\mathbf{R}})^2 + 2\,(c\underline{\mathbf{R}})^{n+1}\right)\mathbf{r}.\end{aligned}$$

To examine $\mathrm{E}[\mathbf{g}_n^T\mathbf{g}_n]$, we express the product as $\mathbf{g}_n^T\mathbf{g}_n = \sum_{k=1}^{n} T_k$ where

$$\begin{aligned}T_k &= {}^k\tilde{\mathbf{t}}_{k-1,k}^T\begin{pmatrix}{}^{k-1}_{\ k}\tilde{\mathbf{R}}_\delta^T & {}^{k-2}_{\ k-1}\tilde{\mathbf{R}}_\delta^T & \cdots & {}^{0}_{\ 1}\tilde{\mathbf{R}}_\delta^T\end{pmatrix}(\underline{\mathbf{R}}^k)^T \\ &\quad\times\left(\underline{\mathbf{R}}\ {}^0_{\ 1}\tilde{\mathbf{R}}_\delta\,{}^1\tilde{\mathbf{t}}_{0,1} + \cdots + \underline{\mathbf{R}}^n\,{}^0_{\ 1}\tilde{\mathbf{R}}_\delta\cdots{}^{k-1}_{\ k}\tilde{\mathbf{R}}_\delta\,{}^k\tilde{\mathbf{t}}_{k-1,k}\right).\end{aligned}$$

Taking expectation and using the assumptions on the noise correlations, we get for $k > 1$,

$$\begin{aligned}\mathrm{E}[T_k] &= \mathrm{Tr}\left[P + \mathbf{b}\mathbf{b}^T\right] + \mathbf{b}^T((c\underline{\mathbf{R}})^{k-2} + (c\underline{\mathbf{R}})^{k-3} + \cdots + I \\ &\quad + I + (c\underline{\mathbf{R}}) + (c\underline{\mathbf{R}})^2 + \cdots + (c\underline{\mathbf{R}})^{n-1-k})\boldsymbol{\rho},\end{aligned}$$

and for $k = 1$, $\mathrm{E}[T_k] = \mathrm{Tr}\left[\mathbf{P} + \mathbf{b}\mathbf{b}^{\mathbf{T}}\right] + \mathbf{b}^T(I + c\underline{\mathbf{R}} + (c\underline{\mathbf{R}})^2 + \cdots + (c\underline{\mathbf{R}})^{n-1-k})\boldsymbol{\rho}$. Repeating this for all the T_k's we get:

$$\begin{aligned}\mathrm{E}[\mathbf{g}_n^T\mathbf{g}_n] &= n\,\mathrm{Tr}\left[\mathbf{P} + \mathbf{b}\mathbf{b}^T\right] + \mathbf{b}^T\left[2\sum_{k=0}^{n-2}(n-k-1)\,(c\underline{\mathbf{R}})^k\right]\boldsymbol{\rho} \\ &= n\,\mathrm{Tr}\left[\mathbf{P} + \mathbf{b}\mathbf{b}^T\right] + \mathbf{b}^T\,(I - c\underline{\mathbf{R}})^{-2}\times \\ &\quad [2(n-1)I - 2nc\underline{\mathbf{R}} + 2\,(c\underline{\mathbf{R}})^n]\,\boldsymbol{\rho}.\end{aligned}$$

Similar tedious calculations lead to the following

$$\begin{aligned}\mathrm{E}[\mathbf{f}_n^T\mathbf{g}_n] &= \left[\sum_{k=0}^{n-1}\mathbf{b}^T(c\underline{\mathbf{R}})^k + \sum_{k=0}^{n-2}(n-k-1)\boldsymbol{\rho}^T(c\underline{\mathbf{R}}^T)^k\right]\mathbf{r} \\ &= \mathbf{b}^T\,(I - c\underline{\mathbf{R}})^{-2}\left[I - c\underline{\mathbf{R}} - (c\underline{\mathbf{R}})^n + (c\underline{\mathbf{R}})^{n+1}\right]\mathbf{r} \\ &\quad + \mathbf{r}^T\,(I - c\underline{\mathbf{R}})^{-2}\,[(n-1)I - nc\underline{\mathbf{R}} + (c\underline{\mathbf{R}})^n]\,\boldsymbol{\rho}.\end{aligned}$$

Plugging all of this back in (25), we get $\mathrm{Tr}\,[Cov\,(\mathbf{e}(n),\mathbf{e}(n))] = \psi n + \omega(n)$, where $\psi, \omega(n)$ are given in (12). This proves the second equality in (13). ■■